2017-03-21

Near-surface distribution of pollutants in coastal waters as assessed by novel polyethylene passive samplers

Aminot, Y

10.1016/j.marpolbul.2017.03.022
Marine Pollution Bulletin
Elsevier BV

Near-surface distribution of pollutants in coastal waters as assessed by novel polyethylene passive samplers

Yann AMINOT[1], Angel BELLES[2], Claire ALARY[2], James W READMAN[1,3]

1. Biogeochemistry Research Centre, Plymouth University, Plymouth, PL4 8AA, United Kingdom

2. IMT Lille Douai, Univ. Lille, EA 4515 - LGCgE - Civil & Environmental Engineering Department, F-59000 Lille, France

3. Plymouth Marine Laboratory, Prospect Place, The Hoe, Plymouth, PL1 3DH, United Kingdom

Abstract

We report a novel and inexpensive method to provide high resolution vertical measurements of temporally integrated organic contaminants in surface and sub-surface waters in polluted coastal environments. It employs a strip of polyethylene deployed as a passive sampler. Verifications are confirmed via conventional spot sample analyses and against Performance Reference Compound (PRC) calibration methods. Analytes targeted include 16 Polycyclic Aromatic Hydrocarbons, 15 personal care products, 8 organophosphorus flame retardants, 4 antifouling 'booster' biocides and 15 n-alkanes. Whilst all contaminants typically revealed homogeneous concentrations from 10 cm to 3 m depth in the selected harbour (less than 30 % variations), many increased sharply at the air-sea interface. The passive sampler was shown to afford better resolution than could be achieved using conventional analytical techniques at the surface microlayer (SML). Whilst hydrophobicity appeared to be a key factor for the enrichment of many determinants, less correlation was found for the emerging contaminants.

Keywords

Sea surface microlayer, passive sampling, surface enrichment, priority and emerging contaminants

Highlights

- 3 m long polyethylene passive samplers exposed in coastal waters
- High resolution subsurface measurements by centimetric slicing of the samplers

- Contaminants concentrated in the sea surface microlayer
- Enrichment factors are compound-dependent

Graphical abstract

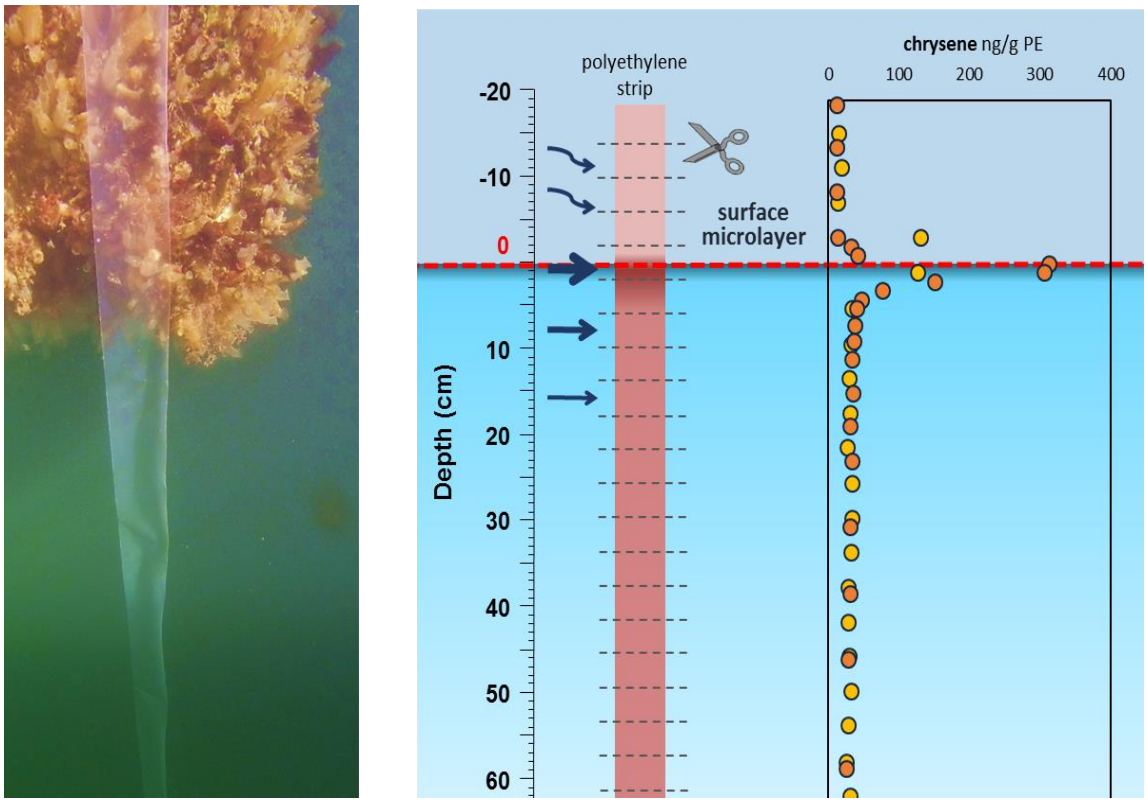

1 Introduction

Coastal and estuarine areas receive contaminants from wastewater discharges and littoral activities such as boating, sea trade and fisheries as well as from upstream inputs through riverine discharges and soil washout (Sumner et al., 2010; Thomas et al., 2001; Aminot et al., 2016). Many contaminants (persistent organic pollutants, antifouling biocides, household and personal care products etc.) are routinely detected in coastal areas where they can affect biota, sorb to sediments and eventually reduce environmental quality and sustainability, especially in regions that from a socio-economic perspective depend on a healthy coastal environment (Bowen et al., 2006). Assessing the distribution of these contaminants in coastal waters provides insights for the understanding of their sources and fate, hence allowing better management of our coastal waters.

There is evidence for the enrichment of contaminants at the sea-atmosphere interface (e.g. Guitart et al., 2007; Wurl and Obbard, 2004). This compartment, also called the sea surface microlayer (SML), is generally accepted to include the top tens to hundreds of µm of the surface layer where physico-chemical and biological properties differ from the subsurface waters. The layer is enriched in low density (< 1 $g.cm^{-3}$) biogenic and anthropogenic organics which influence deposition and volatilisation of both biogenic and anthropogenic chemicals, sea spray formation and has a unique microorganism composition (Cunliffe et al., 2013). Enrichment of pollutants in the SML is therefore likely to have implications in the atmospheric aerosol pollutant load and transport and also the aqueous distributions. The SML has been conventionally collected using various samplers, such as glass plates, mesh screens or rotating drums, each yielding different thicknesses sampled (20 µm - 500 µm), which impairs the intercomparison of enrichment factors (EFs) (Cunliffe et al., 2013). These active sampling methods are also unable to account for temporal variability of the SML unless multiple samples are analysed. Some studies indicate a diurnal pattern of contamination depending on wind and current (Romano and Garabetian, 1996) and its spatial variability where visible slicks further concentrate biogenic and anthropogenic components (Guitart et al., 2004). Passive sampling provides a valuable alternative technique which integrates variations over time (typically 2-3 weeks) and provide a less intrusive sampling method.

Passive samplers have been used for integrated measurements on both sides of the air-sea and sediment-water interfaces, principally for studying fluxes of contaminants (Ruge et al., 2015; Belles et al., 2016a). Recently, 4 to 7 passive samplers were used above and below the surface layer on a custom float to evaluate the profile of selected PAHS (Wu et al., 2016). Even though an accumulation of PAHs near the air-water interface was inferred, the roughness of the waves at the studied sites did not allow data collection of within 6 cm below or above the surface layer, preventing access to the actual SML.

In this paper, we present a novel, simple and inexpensive method to provide high resolution (centimetric) vertical measurement of organic contaminants in the subsurface waters, the SML and in the air above. This is investigated by coupling passive sampling to conventional spot

sampling. Polycyclic aromatic hydrocarbons (PAHs), personal care products (PCPs, including musks and UV filters), organophosphorus flame retardants (OPFRs) and alkanes were targeted. However, the method can be extended to any contaminant amenable to polyethylene passive sampling protocols (Pintado-Herrera et al., 2016). The passive samplers were used to record surface enrichment and subsurface distributions on a centimetre scale in harbour waters. A mathematical model, fitted on the experimental data, was employed to extrapolate the enrichment factors to the desired surface layer thickness (selected at 500 µm) to afford comparison with existing literature on the surface microlayer (SML).

2 Materials and methods

2.1 Chemicals and PE passive sampler preparation

The selected analytes were 16 PAHs (naphthalene, acenaphthylene, acenaphtene, fluorene, phenanthrene, anthracene, fluoranthene, pyrene, benz[a]anthracene, chrysene, benzo[k+f]fluoranthene, benzo[a]pyrene, indeno[1,2,3-c,d]pyrene, benzo[ghi]perylene, dibenz[ah]anthracene), 8 organophosphorous flame retardants (tris(butyl) phosphate [TNBP], tris(isobutyl) phosphate [TIBP], tris(chloroethyl) phosphate [TCEP], tris(2-chloroisopropyl) phosphate [TCIPP], tris(1,3-dichloroisopropyl) phosphate [TDCIPP], tris(2-butoxyethyl) phosphate [TBOEP], tris(phenyl)phosphate [TPHP], 2-Ethylhexyl diphenyl phosphate [EHDPP]), 4 booster biocides (irgarol 1051, terbutryn, chlorothalonil, seanine 211), 2 pesticides used in aquaculture (methyl parathion, deltamethrin), 15 personal care products (tonalide, galaxolide, galaxolidone, cashmeran, lilial, celestolide, phantolide, musk xylene, musk ketone, traseolide, benzophenone, oxybenzone, octocrylene, homosalate, triclosan) and 15 alkanes from C21 to C35.

All chemicals and standards were of the highest purity commercially available and purchased from QMX Laboratories (UK), Sigma-Aldrich (UK) or LGC Standards (UK). Solvents were of HPLC grade and were provided by Rathburn Chemicals Ltd, Walkerburn, UK. Sodium sulfate (> 99 %) was purchased from Fisher Scientific (Loughborough, UK). Ultra-pure water was produced on-site using a Millipore Milli-Q system, with a specific resistivity of 18.2 MΩ cm (25 °C).

Bulk polyethylene (PE) sheets [100 µm thick, Fisher Scientific (Illkirch, France)] were cut into strips (3 m long, 6 cm wide) and were pre-extracted by soaking twice in dichloromethane for 24 h.

Performance reference compounds (PRC, phenanthrene d10 and irgarol d9) were spiked into the material prior to exposure by immersing them in spiked water during 15 days (Belles et al., 2016a). The amount of added compounds in the water was approximately (but accurately measured) 2 µg per gram of spiked polyethylene.

The PE strips were stored at -20 °C in clean metal tins until deployment. A field control sampler was also prepared to measure the initial PRC concentrations and integrate potential contamination during deployment and retrieval operations.

2.2 Site description and deployment

The passive samplers were exposed in Sutton harbour marina (490 berths), situated in Plymouth, UK. The harbour is fitted with lock gates that restrict free flow of sea water to 3 h either side of high tide. Sea water renewal is therefore limited affording the potential for significant vertical stratification of contaminants. Turbulence of the sea surface is also reduced. The tidal lock ensures that a minimum depth of 4m is maintained within the harbour at all times.

The 3 m long PE strips had weights fastened at the bottom and were attached vertically below floating pontoons with 30 cm exposed above the sea surface. Hence, the PS followed the water body vertical movements and its relative position relative to the sea surface was fixed. An additional 30 cm long strip was exposed just below the pontoon as an atmospheric sampler. All samplers were protected from direct sunlight and rainfall by being situated below the pontoon. The sampling area was selected in a sheltered part of the harbour where boat traffic is unlikely to generate high turbulence and spray above the surface. Exposure lasted for 21 days in March 2016. Salinity, temperature, dissolved oxygen and turbidity were monitored on a weekly basis at 50 cm depth intervals using a multiparameter probe (YSI ProDSS) and in subsurface water (50 cm deep) constantly during 3 days. Temperature in the subsurface water (50 cm deep) was also recorded constantly using a temperature logger (Hobo Pendant, Onset).

During the 3 days of continuous measurements, temperature varied between 9 and 10.1 °C following a pattern of warmer days and cooler nights. Salinity was between 32.8 and 33.4 PSU, with no major hourly/daily variation. Turbidity was low at 0.8 ± 0.3 FNU (Formazin Nephelometric Unit); short-lasting increases were observed during the free flow hours, when the current can resuspend settled particles. pH ranged from 8.04 to 8.07, reaching maxima at 19:00 and minima at 07:00. Dissolved oxygen was constantly near saturation between 99 and 107 %.

Spot seawater samples (1 L) were also taken at 6 separate depth intervals (2 m, 1 m, 50 cm, 20 cm, 10 cm, surface layer) during 4 separate days (n=24). Whilst this cannot fully address high temporal variations, it can provide a useful indication of contamination. In addition, in the selected enclosed harbour, tidal variability is substantially reduced, as indicated in supplementary data (Figure S5). Also, contaminant distributions (discussed further) confirmed vertical mixing, except at the surface microlayer, with relatively good agreement between the 4 days of sampling. A weighted 2 L glass bottle, fitted with a metal lever stopcock cap was used to sample the desired depth by triggering the opening of the bottle below the surface. A volume of 500 mL of the surface microlayer was also sampled using a 1 mm mesh laboratory sieve (200 mm diameter) using the mesh screen technique (Cunliffe and Wurl, 2014; Guitart et al., 2004).

The sieve was fully immersed in the water, moved sideways, and slowly lifted out of the water. The sieve was slightly tilted to allow the unwanted subsurface water to decant before collection of the actual sample using a glass funnel and bottle. Approximately 15 mL of surface microlayer water was collected by each immersion, giving a sampled thickness of 400 to 500 µm. Water from all depths, including the SML, was filtered through pre-cleaned Whatman GF/F glass fibre filters (nominal pore size: 0.7 µm) and were stored at -20 °C until extraction.

2.3 Extraction and analysis

Following deployment, the strips were tranported to the laboratory loosely folded in 2 L glass beakers and cleaned with tissues soaked with ultra-pure water. They were sliced using a pre-cleaned razor blade to provide about 40 depth related sub-samples per strip (Figure 1). One strip was cut in variable slices, from approximatively 1 cm above the surface to allow profiling of the sea-surface microlayer, followed by 10 cm sections from 45 cm to 270 cm deep. A second strip was cut at a constant interval of 3.9-4.2 cm from below its attachment (-20 cm) to a depth of 97 cm and every 16.2-16.6 cm from 97 cm to 282 cm. Individual sub-samples were further cut into smaller parts and extaction was performed by soaking the sub-samples three times in 30 mL of dichloromethane during 24 h. Internal standards (11 deuterated PAHs, 2 deuterated OPFRs and 2 deuterated PCPs) were added during the first extraction step. The dichloromethane extracts were then combined and concentrated to 0.3 mL using nitrogen gas flow evaporator.

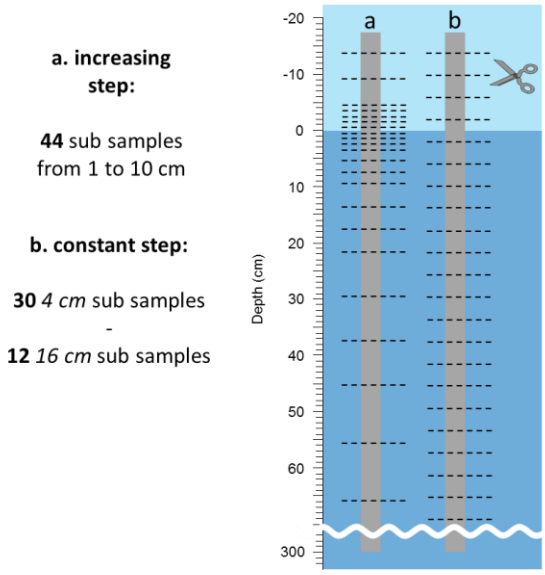

Figure 1. Sub-sampling of the passive sampler strips

The 1 L discreet water samples were extracted by liquid-liquid extraction (LLE) 3 times, each with 50 mL of dichloromethane. Internal standards (11 deuterated PAHs, 2 deuterated OPFRs and 2 deuterated PCPs) were added during the first extraction. The combined extracts were dried using pre-cleaned anhydrous sodium sulphate and were then concentrated to 0.3 mL using rotary evaporation followed by nitrogen blow-down evaporation.

PS and LLE extracts (1 µL) were analysed using an Agilent Technologies 7890A GC system coupled to an Agilent 5975 series Mass Selective detector. A Restek Rxi-1MS (crosslinked poly dimethyl siloxane) capillary column (30 m) with a film thickness of 0.25 µm and internal diameter 0.25 mm was used for separation, with helium as a carrier gas (maintained at a constant flow rate of 1 mL/min). Extracts were injected splitless, with the injector maintained at 250 °C. The oven temperature programme was 110 °C for 2 min and then increased at 5 °C/min to a final temperature of 250 °C, where it was held for 4 min. The mass spectrometer was operated in electron impact mode (at 70 eV) with the ion source and quadrupole analyser temperatures fixed at 230 ◦C and 150 ◦C, respectively. Samples were screened for the analytes and the internal standards using selected ion monitoring (target ions for quantification and confirmation are given in the supplementary material). Prior to sample extract analyses, the system was calibrated using authentic standards. Within each batch of samples, a solvent blank, a standard mixture and a procedural blank were run in sequence for quality assurance purposes. Statistics and modelling were performed using the XLStat software.

2.4 Blank considerations

Because PE samplers can readily be contaminated by air before and after deployment, field and laboratory blanks are essential and quantification of some analytes in blank samplers is not uncommon (McDonough et al., 2016; Ruge et al., 2015). In our study, the potential contamination to the whole strip, contributing to analyte concentrations in ng *per mass of PE* were assessed and quantified in both field and laboratory blanks. All PE samples were consequently blank-corrected by subtracting the average of the field blank concentrations as *ng/g*. Only concentrations greater than three times the standard deviation of the average blank values are reported.

2.5 "Edge effect" evaluations

Our sampling approach is valid only if adjacent centimetric sub-samples of different levels of contamination do not merge, *i.e.* if longitudinal diffusion within the polyethylene strip is negligible. This was evaluated prior to field deployment through a separate experiment termed the "edge effect test". A non-contaminated piece of PE of 15 x 4 cm was stacked between 2 highly PAH contaminated pieces of PE of 1 x 4 cm on its first centimetre and the whole stack was wrapped in foil (Figure S1). PE sheets came from the same 100 µm wide PE batch used for the

actual exposures. After 30 days at room temperature, the central 15 cm piece was sub-sampled every cm and analysed for PAHs using the analytical protocol previously described.

3 Results and discussions

3.1 Depth dependence of the physicochemical parameters

A slight stratification of the water column was observed based on salinity, turbidity and temperature. Salinity was lower in the subsurface (15 cm), and comprised between 31.95 and 33.35 PSU depending on the sampling day (Figure S3). A gradual increase occurred with depth with an additional 0.22 to 0.54 PSU measured at 4 m depth. Assuming a reference salinity of 35 PSU, this suggests a maximum of 8.7 % of potentially contaminated freshwater in the subsurface and between 0.6 and 1.4 % less freshwater at 4 m. The low turbidity measured in the subsurface (0.6 to 1.9 FNU) also increased with depth to values 0.8 to 1.3 FNU higher. The temperature gradient was found to be dependent on the sampling time of the day, with lower values in the subsurface in the morning (0.2 to 0.6 °C less compared to 4 m deep) and warmer waters (+ 0.9 °C) in the surface when the sampling occurred later in the afternoon. This observation agrees with the measurements from the permanently immersed temperature logger indicating water temperature increase during the day (Figure S4). For all parameters, inter-day variations were negligible (Figure S5).

3.2 Edge effect

Only traces of longitudinal diffusion of PAHs were recorded (Figure S2). For 3 and 4-ring PAHs, 2 to 7 % of the amount measured in the first contaminated centimetre diffused into the second cm in 30 days and no 5 and 6-ring PAHs were detected. Naphthalene, the lightest and more diffusive PAH, had 16 to 31 % of the 1st piece amount in the next 3 centimetric pieces (Rusina et al., 2010). It is also noteworthy that this experiment was carried out at room temperature whilst the field exposure was performed in 10 °C waters, which would further limit diffusion in the field. Naphthalene has been previously reported to have the highest diffusion coefficient among PAHs, polychlorinated biphenyls and organochlorine pesticides in a critical review on diffusion coefficients in PE passive samplers (Lohmann, 2012). A recent publication on passive sampling of PCPs and OPFRs reported diffusion coefficients in PE all significantly lower than for naphthalene (Pintado-Herrera et al., 2016). Similarly, the diffusion coefficients calculated for polycyclic musks were lower than for naphthalene in another recent study (McDonough et al., 2016). Our results and the associated diffusion coefficients indicate that little to no longitudinal diffusion will occur during the 3-week field exposures at centimetric resolution.

3.3 Molecules quantified in the samplers and in the water

Among PAHs, dibenz[ah]anthracene was not detected in either PS and LLE water extracts. Benzo[ghi]perylene was not detected in the water extracts. All other PAHs had quantifiable levels (see blank considerations). Naphthalene was not considered as its levels in the field blank were 72 % of the average sample levels. Regarding PCPs and OPFRs, galaxolide, galaxolidone and tonalide exhibited high levels while phantolide, traseolide, musk xylene, musk ketone, triclosan and TBOEP were not detected in PS and LLE water extracts. The relative abundance of polycyclic musks is consistent with the predominant usage of galaxolide and tonalide (Sumner et al., 2010). Trace levels (low ng/L) of cashmeran, lilial, celestolide, oxybenzone, TIBP and TCEP were measured in the LLE water extracts but not in the PS. With lower octanol-water partition coefficients for these compounds, an expected low water-PE partition coefficient is likely to explain this result (Belles et al., 2016b; Lohmann et al., 2012). Among the screened antifouling compounds, only irgarol was detected at trace levels in the LLE water extracts, in agreement with the higher degradability of other antifouling agents (seanine, chlorothalonil) and the ban on irgarol 1051 usage in the UK (Cresswell et al., 2006; Thomas et al., 2003). The pesticides methyl parathion and deltamethrin were not detected. Among alkanes, C21 to C28 were quantified above the limits of detection in PE sampler slices closer to the surface (in both strips). Similarly, high levels of alkanes in the liquid-liquid extraction procedural blanks prevented their accurate analysis in the water sample, with the exception of the surface microlayer extracts.

Below 10 cm depth, little variation was observed in both strips for all compounds, with most RSDs below 30 % and as low as 13 % for fluoranthene and galaxolide (Figure 2 and Figure S6). This observation is in agreement with the water measurements during the 4 monitored days, indicating that the slight stratification observed in physicochemical parameters such as salinity was not reflected in the monitored organics (Figure S3). It also showed an excellent repeatability of the passive sampler measurement (including uptake and extraction protocol). In close vicinity to the surface (within less than 5 centimetres), concentrations of all analytes in the passive samplers showed an acute increase, up to 25 times in the case of phenanthrene. The smaller 1 cm sectioning yielded higher concentrations compared to 4 cm sectioning by integrating more accurately the increase relating to the surface micro-layer. This surface increase allowed molecules below quantifiable levels at deeper levels to be measured near the surface, e.g. benzophenone, TNBP, TCIPP and the alkanes. The concentrations of alkanes below 10 cm (which were below the limit of detection after considering blank corrections) indicate increases as high as 161 and 340 times for C21 between the surface and the subsurface layers for the 4 cm and 1 cm sections, respectively. The analysis of tonalide, galaxolide and galaxolidone was impaired in slices close to the surface owing to increases in chromatogram noise for their selected ions. This also implies an increase in the quantity of co-extractants associated with the surface layer.

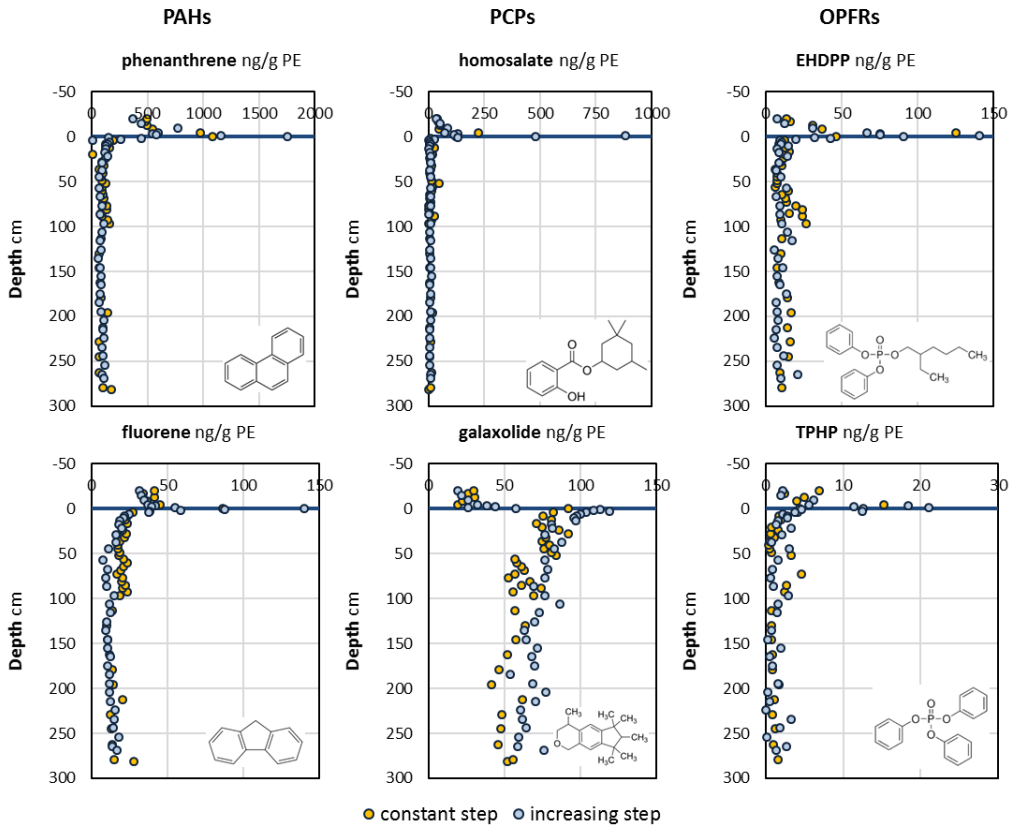

Figure 2. Depth profiles of 6 selected compounds.

Above the water surface, PS concentrations dropped rapidly for most of the analytes to constant values reflecting atmospheric diffusion. As indicated in Figure 3 and Figure S7, the values measured in the separately deployed atmospheric PE sampler confirmed the concentrations obtained in the strip above the surface. However, all PAHs were measured in the atmosphere. Acenaphthylene, acenaphthene, fluorene, phenanthrene, anthracene and fluoranthene were proportion higher in the PS above the surface than below while the trend was the opposite for the 7 heaviest PAH. This directly relates to their volatility and has been previously observed in PE passive samplers (Ruge et al., 2015; Wu et al., 2016).

Among the organophosphorus flame retardants, TCIPP exhibited relatively high concentrations above the surface while concentrations of TPHP and EHDPP above the surface were comparable to subsurface levels. The transformation product galaxolidone was more abundant in the PS above the surface than below, unlike its parent compound galaxolide and the other musk, tonalide. This could relate to dissimilar air/PE and water/PE partitioning coefficients, but no coefficient data is currently available for galaxolidone.

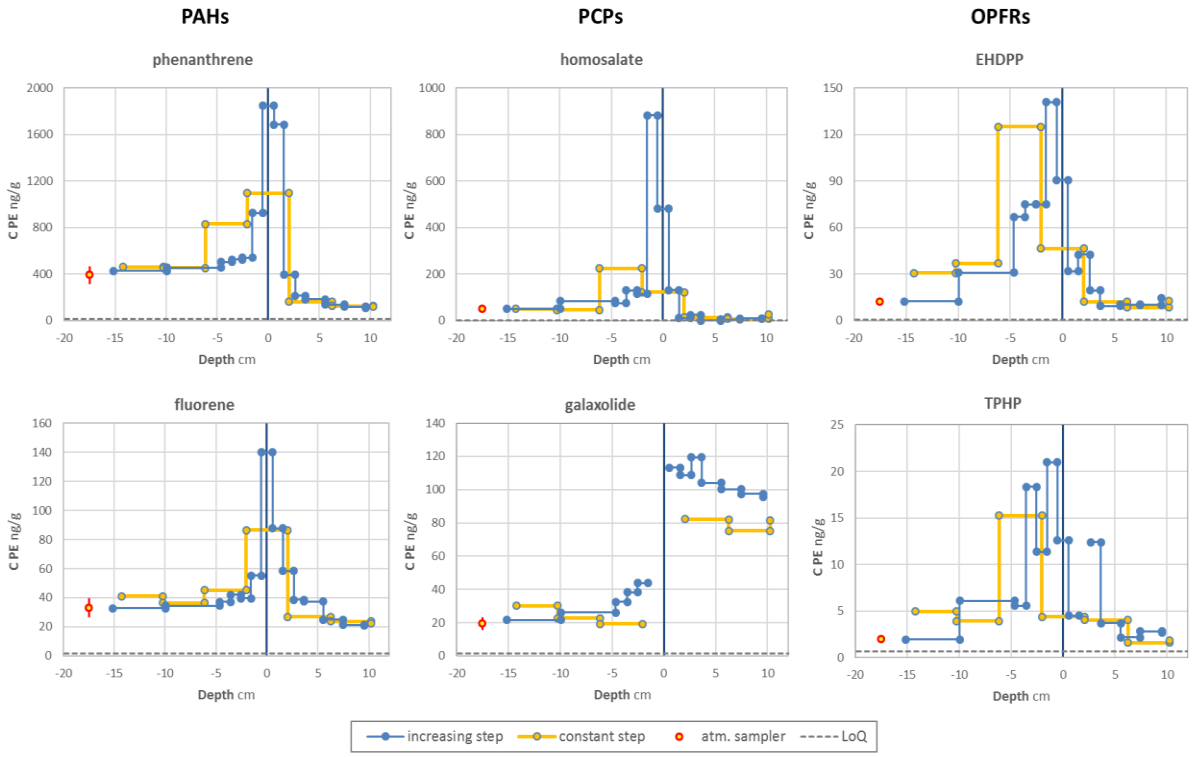

Figure 3. Concentrations in the passive samplers near the air-sea interface for 6 selected compounds.

3.4 In-situ calibration of samplers

To compensate for the variability in contaminant behaviour (hydrophobicity, diffusion, affinity by polymer etc.), we performed an in-situ calibration against water measurements, in which a sampling rate parameter, the alpha ratio, was determined for each compound indicating the specific uptake into the passive sampler.

The matching profiles between the PS extracts and the LLE water extracts in the subsurface waters were used to perform an in-situ calibration and calculate the water concentration of the whole profile from the passive sampling. The overall law for accumulation kinetics of polymeric passive samplers follow the equation (Booij et al., 2007):

$$C_s = C_w K \left(1 - \exp\left(-\frac{Rs}{KV} t\right)\right) \quad (1)$$

Where Cs and Cw are the compound concentrations in PS and water respectively, V is the sampler volume, K is the partitioning coefficient of compounds between water and sampler and Rs is the sampling rate. Two sampling regimes can be distinguished: the accumulation kinetics regime for the short exposure period (t→0) where equation (1) can be simplified to equation (2) and the equilibrium regime (t→∞) where equation (1) can be rearranged as equation (3)

$$C_s = C_w \left(\frac{Rs\, t}{V}\right) \quad (2)$$

$$C_s = C_w(K) \qquad (3)$$

Depending on the sampling regime, the ratio between the sampler concentration and the dissolved concentration refer to the product (Rs.t/V) or refer to the compound distribution coefficient between the water and the sampler (K). This compound specific sampler to water concentration ratio, referred further as the α ratio, is required for deducing the dissolved concentration from the amount of compounds sampled by the polymer strip. In the present approach, α is calculated from the averaged dissolved concentration measured by spot sampling below 50 cm depth (4 days, 3 depths, n=12) and the measured Cs in the same depth range where the concentration is near constant for all compounds (2 strips below 50 cm, n=46). The values and variabilities of dissolved concentration and sampler concentration on this depth range are reported in Table 1 and are used for calculating the corresponding ratio α and its variability (Table 1). The average PS concentrations of both strips below 50 cm was divided by the average water concentration determined by spot sampling at 50, 100 and 200 cm deep on the 4 days sampled. The standard deviations were used to determine the error of α using the propagation of uncertainties. Assuming that Rs and K are independent of depth, α can be used to back-calculate the dissolved concentration of compounds from the measured Cs along the whole depth profile. The minor stratification observed for physicochemical parameters, temperature in particular, supported the assumption of a weak depth-dependence of Rs and K (the temperature at a depth of 15 cm varied between 9 °C and 10.1 °C, with extra variations at 4 m deep of between -0.9 °C and + 0.6 °C). This approach allows the assessment of water concentration profiles of pollutants with a very high spatial resolution for studying the near-surface contamination levels.

Table 1. Average concentrations in subsurface water (averages of depths 50, 100, 200 cm over the 4 days) and average concentrations in the 2 PE strips below 50 cm together with the calculated α ratio.

	C water LLE ng/L	**C PS ng/g**	**α L/g**
PAHs			
Acenaphthylene	1.1 ± 1	3.1 ± 0.7	2.9 ± 3.4
Acenaphthene	1.9 ± 0.8	5.3 ± 1.4	2.7 ± 1.9
Fluorene	2.3 ± 0.4	14.9 ± 4.6	6.5 ± 3.4
Phenanthrene	5.5 ± 0.9	86.8 ± 14.4	15.5 ± 5.3
Anthracene	nd	3.3 ± 1.1	
Fluoranthene	1.9 ± 0.5	94.4 ± 10.7	50.2 ± 18.3
Pyrene	2 ± 0.4	121.9 ± 16.6	62 ± 21.4
Benz[a]anthracene	0.2 ± 0.2	9.8 ± 2.5	46.4 ± 61.7
Chrysene	0.5 ± 0.3	26.2 ± 3.4	53.8 ± 44.9
Benzo[k+f]fluoranthene	nd	10.5 ± 1.0	
Benzo[a]pyrene	0.1 ± 0.1	3.3 ± 1.0	30.5 ± 15.5
Indeno[1,2,3-c,d]pyrene	0.6 ± 0.4	2.2 ± 1.2	3.4 ± 4.2
Benzo[ghi]perylene	nd	2.3 ± 1.6	
PCPs			
lilial	1.2 ± 1.7	nd	
cashmeran	1.3 ± 0.6	nd	
celestolide	0.07 ± 0.04	nd	
galaxolide	5.0 ± 1.1	63.6 ± 10.4	12.6 ± 5

galaxolidone	1.6 ± 0.5	3.4 ± 2	2.1 ± 1.9
tonalide	1.2 ± 0.7	4.4 ± 1.7	3.8 ± 3.8
benzophenone	47.3 ± 55.2	nd	
oxybenzone	2.3 ± 2.2	nd	
homosalate	1.1 ± 0.5	9.4 ± 7.1	8.6 ± 10.3
octocrylene	2.8 ± 1.5	21.9 ± 1	7.8 ± 4.4
OPFRs			
TIBP	2.8 ± 2.1	nd	
TNBP	0.7 ± 0.5	nd	
TCEP	2.6 ± 1.6	nd	
TCIPP	77 ± 20	nd	
TDiCPP	1.3 ± 0.3	nd	
TPHP	3.4 ± 1.7	1.6 ± 0.8	0.4 ± 0.4
EHDPP	15.2 ± 11.5	9.8 ± 3.8	0.6 ± 0.8

The compound-specific α ratio is indicative of the pre-concentration ability of the samplers, regardless of the sampling regime (kinetic accumulation or at equilibrium). Effectively, the pre-concentration of given compounds by a sampler is usually evaluated by comparison of K. However, this approach is only suitable for samplers reaching equilibrium. In our case, α spanned values from 0.4 for TPHP to 62 L/g for pyrene. In other words, the amount of pyrene in a 1 cm PE strip (about 50 mg of PE) corresponds to the sampling of about 3.1 L of water. Compared to the 1 L liquid-liquid extraction, the use of passive sampling led to an improvement in sensitivity for fluoranthene, pyrene, benz[a]anthracene, chrysene, benzo[k+f]fluoranthene and benzo[a]pyrene in addition to afford a spatial resolution down to the centimetric level for all molecules. On the other hand, TPHP and EHDPP, the only OPFRs consistently quantified in the PS, exhibited a low α corresponding to the sampling of only 20 mL of water. For such compounds, direct spot sampling of 1 L offers a better sensitivity, as indicated by the quantification of all OPFRs in the seawater, as high as 77 ± 20 ng/L for TCIPP, while not quantified in the PS. Various OPFRs were qualitatively measured in PE samplers (2.5 x 60 cm, 100 µm thick) exposed during 49 days in a Norwegian urban river (Allan et al., 2013), even though parallel deployment of silicone rubber (SR) samplers indicated a much lower affinity of OPFRs to PE in comparison to SR. More recently, the diffusion coefficients of OPFRs in PE and SR were shown to be 1 order of magnitude lower than for PAHs and lower in PE than in SR (Pintado-Herrera et al., 2016). Our low α value for these compounds can partly be explained by poor water-PE partitioning coefficients (Allan et al., 2013) and/or slow accumulation kinetics implied by the low polyethylene diffusion coefficients (Pintado-Herrera et al., 2016).

3.5 Cross-validation of the *in-situ* calibration

To enhance validation of the in-situ calibration, the calculated dissolved concentration for phenanthrene was compared with the dissolved concentration calculated using the Performance Reference Compound (PRC) calibration method. The PRC calibration method

(which involves the use of PS spiked with deuterated analytes) is frequently reported in the literature but is generally limited to PAH and PCBs. For the non-PAH compounds of our study, which are mainly emerging contaminants, no validated model is available. In addition, appropriate deuterated standards (different labels are required for PRC and analytical internal standards) are scarce restricting PRC options. In the absence of developments specific to the other compounds selected in our study, the PRC approach was used only as a supporting method for phenanthrene. The PRC calibration consists in using the residual amount of tracer compounds spiked in the PE prior to exposure to evaluate the fractional partitioning equilibrium reached for a given compound, deduced from equation (4).

$$f_{eq} = 1 - \frac{C_{PRC}}{C_{PRC\,0}} \qquad (4)$$

where C_{PRC0} and C_{PRC} are the initial and residual amounts of the labelled compounds (PRC) spiked in the PE samplers prior to exposure. According to previous studies (Fernandez et al., 2009), the dissolved concentration of the unlabelled compounds is then deduced from the accumulated amount of analyte (Cs), the fractional equilibrium and the K of the compounds (Equation 5):

$$C_w = \frac{C_{PE}}{K.f_{eq}} \qquad (5)$$

In the present study, K is selected from (Lohmann, 2012). Concentrations of the PRCs phenanthrene d10 and irgarol d9 remained consistent with depth with a RSD of 30 to 40 %, excluding the atmospheric part of the sampler. Relative to the field control, the residual amount of phenanthrene d10 after exposure was 2.4 ± 0.7 % (3.0 ± 1.0 % in the variable cutting step strip) and 17 ± 11 % (19 ± 7 % in the variable cutting step strip) for irgarol d9. Near complete dissipation of phenanthrene indicated a near complete partitioning equilibrium over the 21 days of exposure, which is consistent with the literature (Allan et al., 2009; Belles et al., 2016b; Lohmann, 2012).

Constant residual amounts of PRC throughout the strip supported the assumption of the absence of a depth-dependence of R_S as discussed above. The water concentration derived from the PRC calibration was determined only for phenanthrene (Figure 4) as only irgarol d9 was detected in the PE samplers and not irgarol itself. Its absence probably relates to legislative restrictions on its antifouling use.

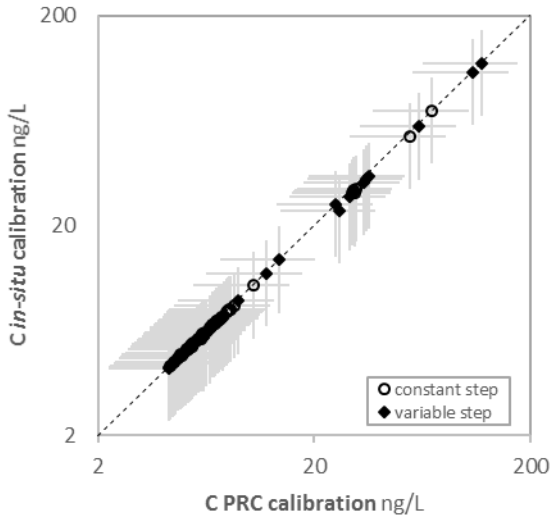

Figure 4. Comparison of the concentrations derived using the PRC and the *in-situ* calibration methods.

For phenanthrene, the two calibration methods indicated practically no difference in the resulting water concentrations with a 99 % and 98 % match on the constant and variable step samplers, respectively. This excellent comparability of the results validates use of the *in-situ* calibration method and confirms the robustness of the PRC approach for compounds where such developments are available.

3.6 Modelling the concentration distribution

A decreasing exponential function showed good agreement with the rapid concentration decrease observed in the PS strips with depth and was chosen as the basis for model development. The chosen model describes the concentration in the PS (C_{PS}; ng/g) as a function of depth (x; cm), as shown in Eq (6):

$$C_{PS}(x) = C_{PS}^{0}.e^{-b.x} + C_{PS}^{depth} \quad (6)$$

where C_{PS}^{0} (ng/g) is the intercept, b the decay constant, and C_{PS}^{depth} (ng/g) the value in depth, typically below 20 cm. The 2 slicing steps were combined in the same dataset by attributing the measured concentration of a PS from a depth range to the range mid-depth ($[C]_{x}^{x+s} = C\left(x + \frac{s}{2}\right)$, where s is the slicing step). These parameters, the coefficient of determination and the depth $x_{1/2}$ for which the surface increase is halved, are given per molecule in table 2. To include the molecules which were not calibrated in the PS (the PAHs not detected in the water extracts), the model was developed using the concentrations in the samplers in ng/g. The conversion to water concentrations as a function of depth in ng/L, in particular C_{PS}^{0} and C_{PS}^{depth},

is straightforward by using the α ratio from table 1 and the modelled water concentrations are given for 3 selected compounds in Figure 5.

Table 2. Parameters of the model. $C_{PS}^{0}$is the intercept, b the decay constant, C_{PS}^{depth} the modelled concentration in depth, $x_{1/2}$ the depth for which the surface increase is halved, R^2 the coefficient of determination and n the number of observations per compound.

	C_{PS}^{0} ng/g	b	C_{PS}^{depth} ng/g	$x_{1/2}$ cm	R^2	n
PAHs						
Acenaphthylene	5 ± 1	-0.21 ± 0.04	3.3 ± 0.1	3.3 ± 0.4	0.87	21
Acenaphthene	7 ± 2	-0.44 ± 0.22	6 ± 0.4	1.6 ± 0.5	0.48	22
Fluorene	158 ± 6	-0.49 ± 0.03	19.8 ± 0.8	1.4 ± 0.1	0.99	22
Phenanthrene	2614 ± 253	-0.54 ± 0.07	92 ± 35	1.3 ± 0.2	0.92	22
Anthracene	18 ± 3	-0.62 ± 0.12	2.4 ± 0.3	1.1 ± 0.3	0.84	22
Fluoranthene	580 ± 34	-0.66 ± 0.05	106 ± 4	1 ± 0.1	0.97	22
Pyrene	973 ± 126	-0.37 ± 0.08	97 ± 24	1.9 ± 0.4	0.85	22
Benz[a]anthracene	61 ± 5	-0.45 ± 0.05	10.7 ± 0.8	1.6 ± 0.2	0.93	22
Chrysene	381 ± 42	-0.44 ± 0.07	32 ± 7	1.6 ± 0.3	0.89	22
Benzo[k+f]fluoranthene	149 ± 11	-0.66 ± 0.07	11.7 ± 1.3	1 ± 0.1	0.95	22
Benzo[a]pyrene	107 ± 24	-0.45 ± 0.15	1.9 ± 3.8	1.5 ± 0.6	0.67	22
Indeno[1,2,3-c,d]pyrene	149 ± 17	-0.74 ± 0.1	4.5 ± 1.7	0.9 ± 0.2	0.90	22
Benzo[ghi]perylene	165 ± 18	-0.69 ± 0.09	5.3 ± 2	1 ± 0.2	0.91	22
PCPs						
galaxolide	20 ± 10	-0.1 ± 0.14	75 ± 7	6.9 ± 1.5	0.19	25
galaxolidone	56 ± 22	-0.57 ± 0.13	2.8 ± 0.3	1.2 ± 0.6	0.84	19
tonalide	16 ± 4	-0.16 ± 0.07	4.4 ± 1	4.2 ± 1.2	0.63	20
benzophenone	404 ± 92	-0.45 ± 0.16	123 ± 19	1.5 ± 0.5	0.75	16
homosalate	1401 ± 92	-0.83 ± 0.07	12.2 ± 9	0.8 ± 0.1	0.97	23
octocrylene	79 ± 9	-0.32 ± 0.07	30 ± 2	2.2 ± 0.3	0.88	22
OPFRs						
TNBP	599 ± 1	-2.24 ± 0	81.6 ± 0.1	0.3 ± 0	1.00	3
TCIPP	29 ± 3	-0.4 ± 0.08	1.8 ± 0.8	1.7 ± 0.4	0.94	12
TPHP	21 ± 3	-0.31 ± 0.08	1.9 ± 0.7	2.3 ± 0.5	0.83	21
EHDPP	170 ± 21	-0.42 ± 0.08	10 ± 3	1.7 ± 0.4	0.88	24
Alkanes						
C21	849483 ± 59381	-0.62 ± 0.06	935 ± 14191	1.1 ± 0.2	0.98	10
C22	510937 ± 38842	-0.52 ± 0.06	0 ± 8859	1.3 ± 0.2	0.97	14
C23	322308 ± 37554	-0.77 ± 0.13	1102 ± 7526	0.9 ± 0.2	0.96	10
C24	254839 ± 14926	-0.94 ± 0.07	2055 ± 1930	0.7 ± 0.1	0.99	13
C25	200540 ± 19900	-1.11 ± 0.15	4703 ± 3333	0.6 ± 0.2	0.99	7
C26	122221 ± 15829	-1.41 ± 0.22	4208 ± 1694	0.5 ± 0.2	0.99	7
C27	128263 ± 28112	-1.58 ± 0.36	5877 ± 1359	0.4 ± 0.2	0.93	14
C28	28228 ± 0	-1.71 ± 0	3540 ± 0	0.4 ± 0	1.00	3

The model achieves a description exceeding 80 % of the variance (R^2>0.8) for a large number of compounds. As previously discussed, the lack of values near the surface for galaxolide,

galaxolidone and tonalide as well as the low number of values for TNBP and some alkanes decrease the quality of the modelling for these compounds.

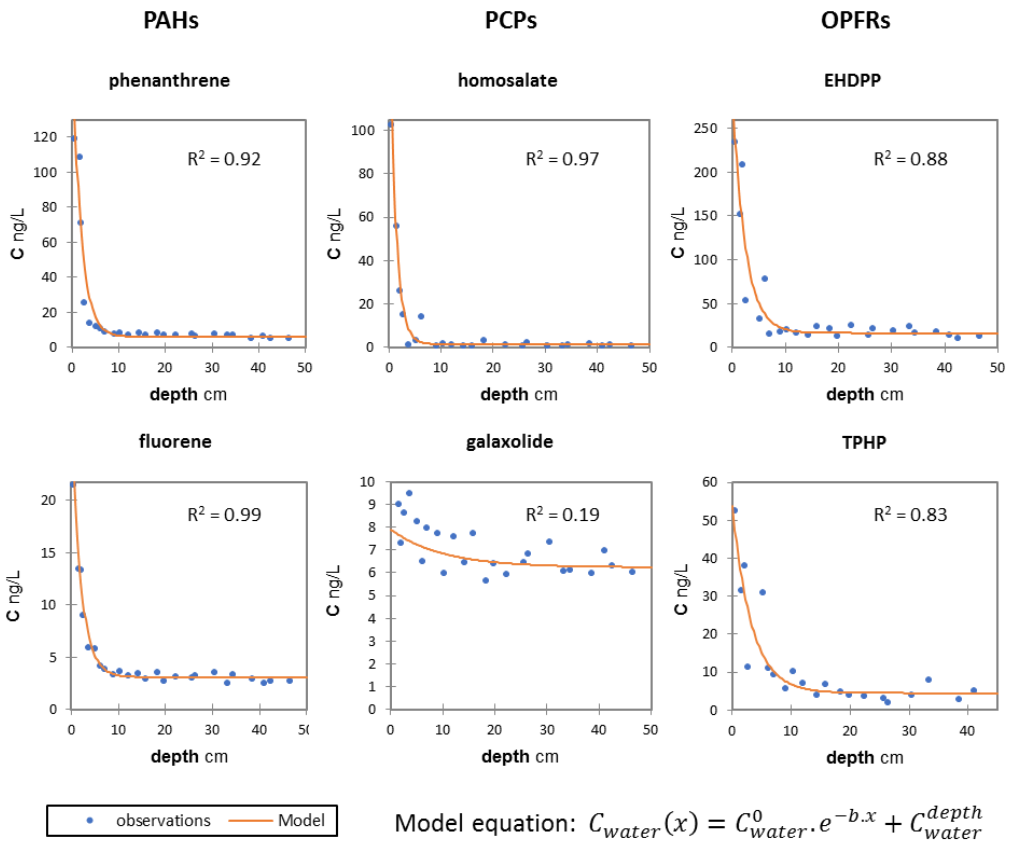

Figure 5. Observed and modelled water concentrations for 6 selected compounds. The parameters of the model are given in table 2.

The decrease in concentrations is sharp from the surface and is halved in less than 2 cm for most compounds. The depth $x_{1/2}$ are homogeneous, indicating that the layer they concentrate in has a similar thickness of under a few centimetres, which is inaccessible to conventional spot sampling techniques. For alkanes, the depth $x_{1/2}$ reduces with increasing carbon number probably relating to their significantly higher hydrophobicity (log Kow of C21 to C28 from 9.8 to 12.91; www.chemicalize.com).

The model also affords calculation of the enrichment factor (EF) between the subsurface and a layer comprised between 0 and less than a millimetre [the surface microlayer (SML)]. For comparison purposes with the literature and our SML sampling, a thickness of 500 µm was selected (depth x=*0.0.025* cm in the model). The EF measured with the 4 cm and the 1 cm slicing step, computed for a 500 µm SML and measured by spot sampling relatively to the average concentrations measured below 20 cm deep are given in table 3. As the alkanes all exhibited

concentrations at depth approximating sampling blank values, their calculations were performed using the limits of detection and should be considered as minimum EFs.

Table 3. Enrichment factors (EF) measured in the passive sampler strips, modelled, and measured by spot sampling. All EFs for alkanes are minimal values as the concentration in subsurface was replaced by the LoD due to higher blank levels.

	Measured by passive sampling	**Measured EF by passive sampling**	**Modelled EF**	**Measured EF by spot sampling**
Thickness	**4 cm**	**1 cm**	**500 µm**	**500 µm**
Acenaphthylene	1.8	2.2	2.6	[0.4 , 1.5]
Acenaphthene	2.0	2.2	2.4	[0.8 , 1.5]
Fluorene	5.4	8.8	11.0	[0.8 , 1.6]
Phenanthrene	12.1	20.3	29.4	[1.3 , 4.1]
Anthracene	3.2	4.5	6.4	<LoD
Fluoranthene	2.8	5.2	7.0	[1.6 , 8.9]
Pyrene	3.4	6.8	9.0	[1.6 , 8.1]
Benz[a]anthracene	3.3	5.9	7.1	[0 , 11.5]
Chrysene	4.8	11.4	14.9	[2.2 , 15.3]
Benzo[k+f]fluoranthene	5.5	11.4	15.2	<LoD
Benzo[a]pyrene	34.7	27.9	35.9	[0 , 8.5]
Indeno[1,2,3-c,d]pyrene	23.8	44.7	62.9	[1.2 , 6.6]
Benzo[ghi]perylene	23.9	48.0	65.0	<LoD
galaxolide	1.3	1.7	1.4	[1.7 , 3]
galaxolidone	2.5	4.2	17.9	[2.4 , 4]
tonalide	1.4	4.4	4.6	[1.5 , 4.9]
benzophenone	1.7	2.1	2.8	[4.1 , 29.5]
homosalate	23.0	90.1	141.4	[2.5 , 5.2]
octocrylene	2.7	3.6	4.2	[2.3 , 4.6]
TNBP	6.2	18.2	46.0	[1.6 , 4]
TCIPP	4.1	11.3	13.6	[1.8 , 3.9]
TPHP	5.9	8.2	8.6	[2.1 , 3.2]
EHDPP	10.5	11.9	15.0	[2.5 , 4.6]
C21	161.3	340.1	471.6	[0.7 , 700.6]
C22	177.8	320.2	448.2	[1.3 , 83.4]
C23	68.0	143.7	217.9	[2.3 , 493.2]
C24	31.7	99.5	163.3	[2.7 , 44.5]
C25	9.7	44.9	79.3	[1 , 1.1]
C26	5.3	26.9	54.3	[0 , 360.8]
C27	3.9	15.5	33.5	[1.3 , 25.6]
C28	0.8	5.9	12.5	[1.2 , 14.2]

The EFs measured by spot sampling over 4 different days appeared to be highly variable (reaching 15 for PAHs, 30 for PCPs, 5 for OPFRs and a minimum of 700 for alkanes, where the LoD was used for the subsurface level), probably owing to the temporal variability of the tidal waters. The EFs derived from the passive sampler strips were in the same order of magnitude,

generally in the higher range of those derived from spot sampling, or higher. The differences observed probably relate to the inherent temporal variability of SML concentrations which would not be accurately measured by the non-integrative spot sampling. It could also be due to either a slight over-estimation of the PS technique or a slight under-estimation using the spot sampling technique. The spot sampling techniques can introduce a methodological bias by physically disrupting the SML and inducing some mixing with the less concentrated subsurface waters. Many dips are necessary to collect a volume of water sufficient to afford analysis and reproducible sub-sampling requires the assumption that the SML is effectively regenerated between trials by water mass drifting (Guitart et al., 2004).

The 'screen' technique used to sample the SML has been employed in previous studies, alongside the glass plate technique. Both techniques resulted in reported EFs spread over a broad range of values (Wurl and Obbard, 2004), sometimes over 3 orders of magnitude. The authors of this review concluded that the heterogeneous nature of the SML and the disparity in sampling techniques complicated comparisons of EF between different regions, or even at different times from a single location. In general, higher EFs were reported in more contaminated waters, typically harbours, where slicks are common (Guigue et al., 2011). Organic matter from waste waters can also induce the formation of a surface active-film able to sorb dissolved contaminants (Guitart et al., 2004).

Regardless of the technique used, the EFs were compound-dependent with values from 2.4 to 65 for PAHs, from 2.8 to 46, generally, for PCPs and OPFRs (141 for homosalate) and above hundreds for the alkanes. For PAHs, EF increased with molecular weight [below 5 for phenanthrene to more than 15 for BaP (Guitart et al., 2007)]. Increase in hydrophobicity (described by log Kow) of heavier PAHs could account for the higher EFs observed (Figure S8). The alkanes, of higher hydrophobicity, show higher EFs but the substitution of their concentration in depth by the limit of detection does not allow a finer comparison, the EF being a minimal value. Regarding PCPs, EFs were in the range of the lightest PAHs, with the exception of the UV filter homosalate (EF of 141) and TNBP (EF of 46). The study for tonalide, galaxolide and galaxolidone was limited owing to their non-detection in the PS slices close to the surface, which impaired modelling. In general, for PCPs and OPFRs, hydrophobicity does not seem to correlate with the increased ratios observed. To date, most of the contaminants studied in the SML are POPs and very little data is available for emerging compounds. Among them, only bisphenol A, octylphenol and nonylphenol have been recently investigated with reported maximal EF values in SML of 17.3, 46.3 and 18.9 respectively (Staniszewska et al., 2015). With a log Kow for octyphenol (5.3) lower than the one for nonylphenol (5.74), their difference in EF does not relate to hydrophobicity despite very similar structures. Overall, our study indicated that only for PAHs a mild correlation existed with log Kow (R^2=0.55), indicating that the SML enrichment does not exclusively result from a partition process between the subsurface waters and an 'octanol-like' surface layer.

Elevated co-extractants detected in samples from the near surface passive samplers indicate a greater molecular complexity in, surface compared to subsurface waters. This is likely to induce more interactions specific to chemical properties. Previous work has shown the SML enrichment of lipids and carbohydrates (Cunliffe and Murrell, 2009; Frka et al., 2009), constituents of the so-called dissolved organic matter pool known to bind to some organic micropollutants (King et al., 2007). pH was also found to decrease nearly 0.2 units in the SML (Zhang et al., 2003). For a compound exhibiting a pK_A in this pH change range, a 0.2 unit pH variation results in a 10-15 % change in the re-partition between the acid and basic form of the compound (estimated from www.chemicalize.com on oxybenzone). The same study also observed a significant increase in suspended solids (SS) in the SML, potentially concentrating compounds prone to SS partition.

As hydrophobicity does not appear to be the key factor in the distribution of hetero-atom containing emerging compounds between the SML and the subsurface waters, further studies are required to unravel the compound specific enrichments observed.

Conclusions

Spot and passive sampling techniques both afford differing advantages and limitations. This research shows that passive sampling using polyethylene strips is a suitable technique to integrate inherent temporal variability of pollutant concentrations both in the SML and sub-surface waters of contaminated harbour environments. Sub-sampling of deployed and inexpensive polyethylene strips offered a high vertical resolution of temporally integrated contamination from the air-sea interface to a depth of approximately 3m. Whilst the accumulation of organic contaminants in polyethylene varies significantly between compounds according to hydrophobicity, diffusion or affinity to the polymer, our preliminary studies using spot sample comparison and PRC calibration against phenanthrene d10 indicate generally good agreement and calculation of an in-situ sampling ratio (alpha) offers potential to develop its application to a broader range of compounds. The PE sampler can also be extended in terms of depth and can potentially be applied to other environmentally susceptible locations, wherever an appropriate structure is available to suspend the device (e.g. a buoy).

Acknowledgments

This study was financially supported by the SEA-on-a-CHIP project, funded from European Union's Seventh Framework Programme (FP7-OCEAN-2013) under grant agreement No.614168.

References

Allan, I.J., Booij, K., Paschke, A., Vrana, B., Mills, G.A., Greenwood, R., 2009. Field Performance of Seven Passive Sampling Devices for Monitoring of Hydrophobic Substances. Environ. Sci. Technol. 43, 5383–5390. doi:10.1021/es900608w

Allan, I.J., Harman, C., Ranneklev, S.B., Thomas, K.V., Grung, M., 2013. Passive sampling for target and nontarget analyses of moderately polar and nonpolar substances in water. Environ. Toxicol. Chem. 32, 1718–1726. doi:10.1002/etc.2260

Aminot, Y., Le Menach, K., Pardon, P., Etcheber, H., Budzinski, H., 2016. Inputs and seasonal removal of pharmaceuticals in the estuarine Garonne River. Mar. Chem., 13th International Estuarine Biogeochemistry Symposium (IEBS) - Estuaries Under Anthropogenic Pressure 185, 3–11. doi:10.1016/j.marchem.2016.05.010

Belles, A., Alary, C., Criquet, J., Ivanovsky, A., Billon, G., 2016a. Assessing the transport of PAH in the surficial sediment layer by passive sampler approach. Sci. Total Environ. doi:10.1016/j.scitotenv.2016.10.198

Belles, A., Alary, C., Mamindy-Pajany, Y., 2016b. Thickness and material selection of polymeric passive samplers for polycyclic aromatic hydrocarbons in water: Which more strongly affects sampler properties? Environ. Toxicol. Chem. 35, 1708–1717. doi:10.1002/etc.3326

Booij, K., Vrana, B., Huckins, J.N., 2007. Chapter 7 Theory, modelling and calibration of passive samplers used in water monitoring.

Bowen, R.E., Halvorson, H., Depledge, M.H., 2006. The oceans and human health. Mar. Pollut. Bull., The Oceans and Human Health 53, 541–544. doi:10.1016/j.marpolbul.2006.08.001

Cresswell, T., Richards, J.P., Glegg, G.A., Readman, J.W., 2006. The impact of legislation on the usage and environmental concentrations of Irgarol 1051 in UK coastal waters. Mar. Pollut. Bull. 52, 1169–1175. doi:10.1016/j.marpolbul.2006.01.014

Cunliffe, M., Engel, A., Frka, S., Gašparović, B., Guitart, C., Murrell, J.C., Salter, M., Stolle, C., Upstill-Goddard, R., Wurl, O., 2013. Sea surface microlayers: A unified physicochemical and biological perspective of the air–ocean interface. Prog. Oceanogr. 109, 104–116. doi:10.1016/j.pocean.2012.08.004

Cunliffe, M., Murrell, J.C., 2009. The sea-surface microlayer is a gelatinous biofilm. ISME J. 3, 1001–1003. doi:10.1038/ismej.2009.69

Cunliffe, M., Wurl, O., 2014. Guide to Best Practices to Study the Ocean's Surface. Occasional publications of the Marine Biological Association of the United Kingdom, Plymouth.

Fernandez, L.A., Harvey, C.F., Gschwend, P.M., 2009. Using Performance Reference Compounds in Polyethylene Passive Samplers to Deduce Sediment Porewater Concentrations for Numerous Target Chemicals. Environ. Sci. Technol. 43, 8888–8894. doi:10.1021/es901877a

Frka, S., Kozarac, Z., Ćosović, B., 2009. Characterization and seasonal variations of surface active substances in the natural sea surface micro-layers of the coastal Middle Adriatic stations. Estuar. Coast. Shelf Sci. 85, 555–564. doi:10.1016/j.ecss.2009.09.023

Guigue, C., Tedetti, M., Giorgi, S., Goutx, M., 2011. Occurrence and distribution of hydrocarbons in the surface microlayer and subsurface water from the urban coastal marine area off Marseilles, Northwestern Mediterranean Sea. Mar. Pollut. Bull. 62, 2741–2752. doi:10.1016/j.marpolbul.2011.09.013

Guitart, C., Frickers, P., Horrillo-Caraballo, J., Law, R.J., Readman, J.W., 2008. Characterization of sea surface chemical contamination after shipping accidents. Environ. Sci. Technol. 42, 2275–2282.

Guitart, C., García-Flor, N., Bayona, J.M., Albaigés, J., 2007. Occurrence and fate of polycyclic aromatic hydrocarbons in the coastal surface microlayer. Mar. Pollut. Bull. 54, 186–194. doi:10.1016/j.marpolbul.2006.10.008

Guitart, C., García-Flor, N., Dachs, J., Bayona, J.M., Albaigés, J., 2004. Evaluation of sampling devices for the determination of polycyclic aromatic hydrocarbons in surface microlayer coastal waters. Mar. Pollut. Bull. 48, 961–968. doi:10.1016/j.marpolbul.2003.12.002

King, A.J., Readman, J.W., Zhou, J.L., 2007. Behaviour of polycyclic aromatic hydrocarbons in dissolved, colloidal, and particulate phases in sedimentary cores. Int. J. Environ. Anal. Chem. 87, 211–225. doi:10.1080/03067310601025189

Lohmann, R., 2012. Critical Review of Low-Density Polyethylene's Partitioning and Diffusion Coefficients for Trace Organic Contaminants and Implications for Its Use As a Passive Sampler. Environ. Sci. Technol. 46, 606–618. doi:10.1021/es202702y

Lohmann, R., Booij, K., Smedes, F., Vrana, B., 2012. Use of passive sampling devices for monitoring and compliance checking of POP concentrations in water. Environ. Sci. Pollut. Res. 19, 1885–1895. doi:10.1007/s11356-012-0748-9

McDonough, C.A., Helm, P.A., Muir, D., Puggioni, G., Lohmann, R., 2016. Polycyclic Musks in the Air and Water of the Lower Great Lakes: Spatial Distribution and Volatilization from Surface Waters. Environ. Sci. Technol. 50, 11575–11583. doi:10.1021/acs.est.6b03657

Pintado-Herrera, M.G., Lara-Martín, P.A., González-Mazo, E., Allan, I.J., 2016. Determination of silicone rubber and low density polyethylene diffusion and polymer-water partition coefficients for emerging contaminants. Environ. Toxicol. Chem. SETAC. doi:10.1002/etc.3390

Romano, J.-C., Garabetian, F., 1996. Photographic records of sea-surface microlayers as a survey of pollution daily rhythm in coastal waters. Mar. Environ. Res. 41, 265–279. doi:10.1016/0141-1136(95)00019-4

Ruge, Z., Muir, D., Helm, P., Lohmann, R., 2015. Concentrations, Trends, and Air–Water Exchange of PAHs and PBDEs Derived from Passive Samplers in Lake Superior in 2011. Environ. Sci. Technol. 49, 13777–13786. doi:10.1021/acs.est.5b02611

Rusina, T.P., Smedes, F., Klanova, J., 2010. Diffusion coefficients of polychlorinated biphenyls and polycyclic aromatic hydrocarbons in polydimethylsiloxane and low-density polyethylene polymers. J. Appl. Polym. Sci. 116, 1803–1810. doi:10.1002/app.31704

Staniszewska, M., Koniecko, I., Falkowska, L., Krzymyk, E., 2015. Occurrence and distribution of bisphenol A and alkylphenols in the water of the gulf of Gdansk (Southern Baltic). Mar. Pollut. Bull. 91, 372–379. doi:10.1016/j.marpolbul.2014.11.027

Sumner, N.R., Guitart, C., Fuentes, G., Readman, J.W., 2010. Inputs and distributions of synthetic musk fragrances in an estuarine and coastal environment; a case study. Environ. Pollut. 158, 215–222. doi:10.1016/j.envpol.2009.07.018

Thomas, K.V., Fileman, T.W., Readman, J.W., Waldock, M.J., 2001. Antifouling Paint Booster Biocides in the UK Coastal Environment and Potential Risks of Biological Effects. Mar. Pollut. Bull. 42, 677–688. doi:10.1016/S0025-326X(00)00216-2

Thomas, K.V., McHugh, M., Hilton, M., Waldock, M., 2003. Increased persistence of antifouling paint biocides when associated with paint particles. Environ. Pollut. 123, 153–161. doi:10.1016/S0269-7491(02)00343-3

Wu, C.-C., Yao, Y., Bao, L.-J., Wu, F.-C., Wong, C.S., Tao, S., Zeng, E.Y., 2016. Fugacity gradients of hydrophobic organics across the air-water interface measured with a novel passive sampler. Environ. Pollut. 218, 1108–1115. doi:10.1016/j.envpol.2016.08.064

Wurl, O., Obbard, J.P., 2004. A review of pollutants in the sea-surface microlayer (SML): a unique habitat for marine organisms. Mar. Pollut. Bull. 48, 1016–1030. doi:10.1016/j.marpolbul.2004.03.016

Zhang, Z., Liu, L., Liu, C., Cai, W., 2003. Studies on the sea surface microlayer: II. The layer of sudden change of physical and chemical properties. J. Colloid Interface Sci. 264, 148–159. doi:10.1016/S0021-9797(03)00390-4